Resistance anomaly near phase transition in confined ferromagnetic nanowires

M. Venkata Kamalakar* and A. K. Raychaudhuri†
DST Unit for Nanosciences, Department of Material Sciences, S. N. Bose National Centre for Basic Sciences, Block-JD, Sector-III, Salt Lake, Kolkata 700098, India
(Received 5 August 2010; published 12 November 2010)

In this paper we report the study of the resistance anomaly close to the ferromagnetic phase transition temperature T_C in Ni nanowires. The electrical resistance measurements on well characterized Ni nanowires of diameters down to 20 nm were carried out over an extensive temperature range (4–675 K), which encompasses the region close to T_C (reduced temperature $|t| \leq 10^{-2}$). The wires were grown in porous alumina templates by electrodeposition and the experiments were carried out by retaining the wires in the templates. The strain that is generated by retaining the wires in the templates was estimated and its effect was considered in the analysis. The data analysis done in the framework of critical behavior of resistance near T_C reveals that the critical behavior persists even down to the lowest diameter wire of 20 nm. However, there is a suppression of the critical behavior of the resistivity as characterized by the critical exponent α and the amplitude of the derivative $\frac{d\rho(T)}{dT}$ at T_C. We observed a considerable suppression of T_C (as determined from resistance data). The shift in T_C as well as the suppression of $\frac{d\rho(T)}{dT}$ are explained as arising from finite size effects.

DOI: 10.1103/PhysRevB.82.195425 PACS number(s): 73.63.−b, 75.40.Cx

I. INTRODUCTION

Resistivity (ρ) of a metallic nanowire is a topic of considerable current interest. In addition to effects such as quantum transport, even in the regime of classical transport there are a number of effects that make them differ from the bulk metals. In the past we have investigated experimentally the electrical resistivity in fcc metal nanowires (including Ni) with diameter as low as 13 nm.[1,2] Phenomena such as residual resistivity arising from surface scattering, electron-phonon interactions, and temperature dependent resistivity with a size dependent Debye temperature, fluctuations and size instability,[3] and also spin scattering (in magnetic nanowires) (Ref. 2) have been investigated. Measurement on single high quality monocrystalline nanowire[4] of Ni has been investigated down to 3 K to validate the conclusions made from measurements done by retaining wires within arrays. These experiments established the extent to which the concepts and theories developed for bulk conventional metals can be applied to metal nanowires.

In this paper we explore an interesting and rather fundamental issue in ferromagnetic nanowires (Ni), namely, what happens to the resistance anomaly near the ferromagnetic transition temperature T_C upon size reduction. Bulk Ni, near the ferromagnetic transition temperature T_C, shows a clear resistance anomaly that is associated with critical point phenomena.[5] In this paper we report an investigation of the resistance anomaly in Ni nanowires of diameter ranging from 200 to 20 nm near the T_C, through measurement of electrical resistance (R) in the temperature range $4 \leq T \leq 675$ K. The measurement, made close to the critical temperature T_C ($|t| \leq 10^{-2}$, where $t = \frac{T-T_c}{T_c}$), allows us to investigate whether the critical anomaly in R persists even in nanowires with diameters less than or comparable to the correlation length. In the range of temperature investigated, we do come close enough to T_C, such that the growing spin correlation length can be truncated by the finite size of the sample. It is noted that the effect of finite size on resistance anomaly has been investigated before in thin films.[6] Shift in the transition temperature of ferromagnetic metals to investigate the role of finite size effects has been studied before in films and nanowires using magnetization measurements.[6,7] Here, we report the investigation of finite size effects on resistance anomaly at the critical region in ferromagnetic nanowires.

In a ferromagnetic nanowire, the relative size of the domain wall width (d_W) with respect to the diameter (d) decides the magnetic nature of the wire. If $d < \sqrt{\pi} d_W$ and length $\gg d_W$, the wire has one dimensional magnetic behavior.[8] In a one-dimensional ferromagnetic nanowire there are two principal anisotropic energies (the shape anisotropy energy and the magnetocrystalline anisotropy) which determine the easy axis for magnetization. In nickel nanowire, the shape anisotropy energy is at least one order more than the magnetocrystalline anisotropy energy. As a result the easy axis is along the axis of the wire. The magnetization can have either of the two directions and the magnetization dynamics is determined by the potential barrier between the two stable orientations. In the diameter range < 35 nm, the spin structure in Ni nanowires can become predominantly one dimensional.[8,9]

Resistivity anomaly near a continuous transition has been associated with the specific heat anomaly (C) (Ref. 10) so that $\frac{d\rho}{dT} \propto C$. This has been proved in precision measurements on Ni (Refs. 11 and 12) and Gd.[13] The critical exponent α determined from both specific heat as well as resistivity anomaly were found to be similar in bulk Ni and Gd. There is no theory or experiment that has addressed the validity of the above theory[10] in the size range of nanowires investigated here, where the effects of finite size should be visible. We note that the premises of the theory depends on short-range spin correlation which we believe may be sufficiently unaltered in these wires and thus there may be reason enough to assume the validity of the above theory. However, our analysis of the results, which we present here, in no way depends on the validity of the above relation. We have inves-

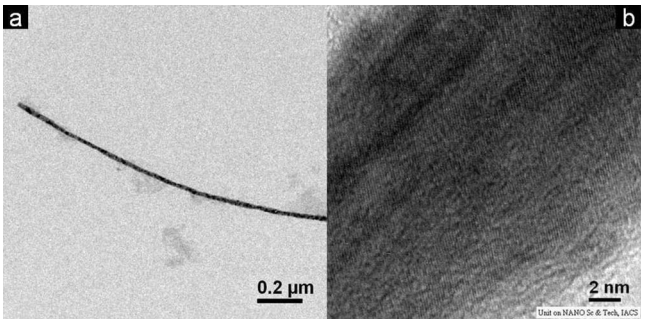

FIG. 1. (a) TEM image of a 20 nm diameter nickel nanowire. (b) HRTEM image of an edge of a 20 nm diameter nickel nanowire.

tigated what happens to the T_C as well as the resistance anomaly close to T_C.

We expect that in the discussed size range two effects may become operative in nanowires. The first effect is related to the issue of finite size. Such an effect can describe the shift of the ferromagnetic T_C as a function of size.[14] It can also reduce the amplitude of the critical phenomena. In the context of ferromagnetic nanowires, this particular point (shift of T_C with size) has been looked into in only one study through determination of T_C from magnetization measurements.[7] The other issue is related to dimensional crossover due to one dimensional nature of the spin which one can infer from the magnetization behavior including relaxation of magnetization. In a recent experiment we found that even the low-frequency spin fluctuations that show up as $1/f$ noise also shows clear signature of the one-dimensional behavior.[9] However, it has not been explored whether that can modify the critical region and whether the resistance anomaly seen in the critical region has signature of this crossover to a quasi one-dimensional behavior.

It is noted that doing this type of experiments, with the nanowires embedded in the template, does have limitations, some of which we elaborate below. The first limitation arises because these experiments done to such high temperatures need to be done by retaining them in the alumina templates in which they are grown. The type of single wire samples made from freestanding nanowires with lithographically fabricated electrodes are not stable up to the temperatures as high as the T_C. The confinement in the template does impose uniaxial strain due to large mismatch in thermal expansion coefficients. This can affect the nature of critical behavior. The second limitation arises because of inhomogeneous strain in the nanowires which can broaden the transition region. We try to address these issues in the data analysis and note that the inference from the experiment will be affected by these limitations.

Doing the quantitative estimation of resistance anomaly in nanowires due to critical phenomena has a fundamental limitation. This is because as the size is reduced, not only does the critical part of the resistance change, there is a significant change in the noncritical part as well. The noncritical part changes because the residual resistivity as well as the temperature dependent part both change. In the nanowires, both of these are enhanced (discussed below) and can suppress the contribution from the critical part. A good estimation of both would need measurements done to rather low temperature (4 K) and in this investigation this was done so that uncertainties in analysis of data arising from the noncritical part of resistivity can be minimized.

II. EXPERIMENTAL

A. Synthesis and characterization

The synthesis of nickel nanowires was done by electrodeposition of nickel from a $1M$ $NiCl_2 \cdot 7H_20$ solution into the pores of nanoporous anodic alumina membranes having thickness in the range 50–60 μm. The diameters of pores inside the membranes have a very narrow size distribution (rms value $< \pm 5\%$) and the wires grown in them have nearly the same diameter as that of the pore. The details of the method of preparation have been given elsewhere.[15,16] X-ray diffraction (XRD) of the nickel filled membranes revealed fcc structure of the nickel nanowire arrays with lattice constant of 3.54 Å (the lattice constant of bulk Ni is 3.52 Å). Energy dispersive spectroscopy further confirmed the purity of the nanowires. A transmission electron micrograph and high resolution transmission electron microscope (HRTEM) image of 20 nm diameter nanowires are shown in Figs. 1(a) and 1(b) respectively. To improve the homogeneity and to reduce the resistance due to grain boundary contribution, the nanowires were annealed at 670 K for 24 h in a vacuum of better than 10^{-6} mbar. XRD pattern of the Ni nanowires after vacuum annealing did not show any peaks of NiO ruling out any oxidation of the samples. The annealing increased the average grain size and in most samples the average grain diameter (as estimated from XRD line width) is approximately similar to wire diameters (see Table I). The annealing also made the wires stable against resistance drifts during the measurement. In addition to structural characterization, the wires were characterized magnetically for $T \leq 300$ K, to establish that the wires have well defined ferromagnetic state. The investigation of magnetic behavior is not

TABLE I. Characterization results.

Diameter (nm)	Grain size (nm)	Microstrain	Coercivity (Oe)	Residual resistivity (Ω m)	Debye temperature θ_R (K)
200	216	0.004	100	1.74×10^{-8}	329
100	109	0.004	120	2.78×10^{-8}	312
55	47	0.006	116	8.24×10^{-8}	281
20	30	0.007	113	1.19×10^{-7}	224

within the scope of the paper and we do not discuss them here. The nanowires showed characteristic hysteresis curves. The coercivities determined from hysteresis loops are summarized in Table I. The coercivities of the wires are comparable although the diameter of the wires varied by one order. The density of nanowires are more or less the same depending upon the diameter and does not appear to have much influence on the coercivity. The coercivity rather depends on how the easy axis of magnetization aligns with respect to the wire length. The nanowires used in this experiment are synthesized by dc electrodeposition mechanism and are polycrystalline with the value of coercivity remaining almost the same as the diameter is changed. This is in contrast to the nanowires synthesized by pulsed deposition,[2,4] where the wires are oriented and are single crystalline. In such wires, where there is alignment of the easy axis of magnetization with the length of the wire, the coercivity can assume much larger values (≈ 900 Oe) as the wire diameter is reduced to 20 nm. A reasonable measure of the inhomogeneous strain (microstrain) as well as the crystallographic grain size can be obtained from the x-ray linewidth measurements. The linewidth in nanowires is determined by the finite grain size along with the strain inhomogeneity. The contribution of both of these can be separated out from the linewidth measurements using the Williamson Hall plot,[17] which is obtained by measuring the linewidth for reflections from different crystallographic planes (hkl). The grain size and microstrain (strain inhomogeneity) shown in Table I have been obtained from this analysis.

B. Resistance measurement

The resistance of the bulk nickel wire (diameter = 50 μm) was measured by four probe method while for the nanowire arrays a pseudo four probe technique[1,2] was used by retaining the wires inside the template. The leads were attached using high temperature silver epoxy. For measurement, a phase sensitive detection technique using a low frequency ac signal was used and the samples were kept in a high vacuum (10^{-6} mbar) in a specially designed high temperature resistivity measurement setup.[16] The temperature was measured and controlled by a temperature controller (with PT100 sensor) allowing resolution and control to a millikelvin. Close to T_C, the resistance of the samples was measured at a slow ramp of 0.1 K/min.

III. RESULTS

We first show the results from the experiment and then analyze the data near T_C to quantify the resistance behavior near the critical region. Figure 2 shows the resistivity data obtained in the nanowire arrays (normalized with the value of ρ at 300 K) along with that of the bulk sample (the 50 μm wire) in the complete temperature range of 4–675 K. The resistivity data of some of the samples (the 50 μm wire, 200 nm and 55 nm nanowires) are shown in the inset of the figure. Other data were left out for clarity.

The data in Fig. 2 show the resistance anomaly at the T_C. The resistance anomaly near T_C arises from magnetic origin

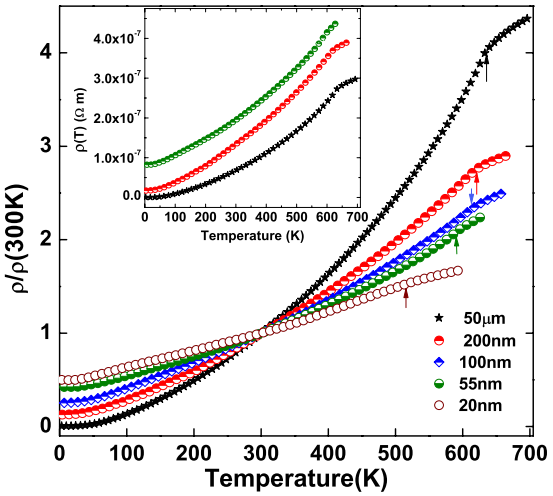

FIG. 2. (Color online) Normalized plot of ρ vs T for nickel nanowires of varying diameters in temperature range $4 \leq T \leq 675$ K. The inset shows the absolute value of the resistivity ρ vs T for some of the wires.

and is related to the critical behavior. In addition to that, the resistivity also has a noncritical part (nonmagnetic part) consisting of a temperature independent residual resistivity (ρ_0) as well as a temperature dependent part arising from electron-phonon interactions. Both these parts change as the diameter of the nanowires change. The measurement as well as analysis of resistivity of Ni nanowires from 3 to 300 K and its diameter dependence have been discussed in details by us before.[2] The analysis of the resistivity data measured in arrays (in alumina templates) were validated by experiments carried out on single monocrystalline nanowire.[4] The focus of this paper is to discuss the critical behavior associated with the resistance anomaly near T_C. As a result we do not discuss here the analysis of the data for $T < 300$ K to avoid repetition and refer to the earlier publications,[1,2] which also discuss in details the method to convert resistance data to resistivity data.

The low temperature part ($T < 300$ K) of the resistivity ρ for the nanowire arrays need to be analyzed to characterize the noncritical part of the resistivity which is also present at T_C along with the critical part. Briefly, our analyses done in earlier publications[1,2] have shown that the residual resistivity (ρ_0) arises mainly from surface scattering and it increases as the diameter decreases (see Table I). The temperature-dependent part till 250 K (Ref. 4) mainly arises from electron-phonon interactions, analyzed using a Debye temperature (θ_R), which decreases as the diameter decreases (see Table I for a tabulation of θ_R from our data). We note that the θ_R is reduced to nearly 0.45 times of the bulk value in the lowest diameter wire. The reduction in θ_R enhances the temperature dependent electron-phonon contribution. Due to the fact that the major contribution of the noncritical part to ρ arises from the electron-phonon interactions, close to T_C, the temperature being $\gg \theta_R$, the noncritical part has a linear temperature dependence. We used this important information in the analysis of the data discussed later on. The enhanced resistivity that arises in the nanowires both due to enhancement of the residual resistivity and also the electron-phonon

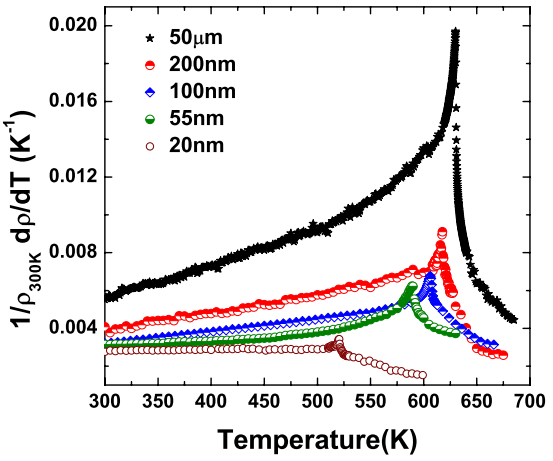

FIG. 3. (Color online) Plot of $\frac{1}{\rho_{300\ \mathrm{K}}}\frac{d\rho}{dT}$ vs T for nickel nanowires as compared to bulk. The transition temperature T_C can be clearly identified.

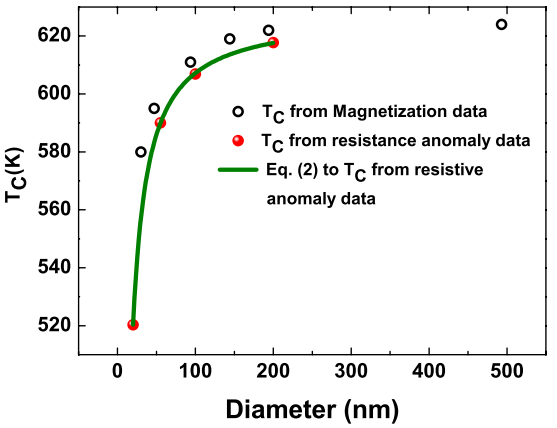

FIG. 4. (Color online) The variation in T_C with diameter studied from resistance anomaly (this work) being compared to that obtained from magnetic measurements (Ref. 7). The line through the data shows fit of the data (resistance anomaly data) to the finite size scaling, Eq. (2).

part, has the effect of reducing the relative contribution of the critical scattering from the spin fluctuations near the critical region as the size is reduced.

As mentioned in Table I, the decrease in Debye temperature (θ_R) with decreasing wire diameter follows a particular trend which we established in our previous work.[2] The electron-phonon interaction contribution to the resistivity increases as the wire diameter is decreased due to the lowering in Debye temperature. Such a decrease in the θ_R is expected to arise from an enhanced effective surface area (an enhancement in the surface to volume ratio) with reducing wire diameter. An enhanced number of surface atoms having missing bonds would give rise to effective lowering of the elastic modulus and hence a lower effective Debye temperature. The effect of presence of template as it appears from the comparison of data taken on a single free nanowire[4] is to modify the surface and increase the effective Debye temperature more.

In Fig. 2, the T_C as determined by quantitative analysis, described later on, are marked by arrows (the approximate value of T_C is taken as the temperature where the derivative of resistance shows a maximum). It can be seen that the anomaly in the resistance reduces as the diameter is reduced (along with a distinct reduction in T_C). However, the anomaly, though reduced, is present even in the wire with the smallest diameter. To accentuate the anomaly in ρ we show in Fig. 3 the derivative of the resistance ($\frac{1}{\rho_{300\ \mathrm{K}}}\frac{d\rho}{dT}$) as a function of T. The presence of the distinct feature in the derivative near T_C is present in all the wires, though much reduced in the wires of smaller diameter. It is seen that the T_C is reduced as diameter d is reduced. The dependence of T_C on wire diameter d is shown in Fig. 4. The reduction in T_C (as determined from the resistance data) with diameter d is very similar to that obtained from magnetization measurements[7] also shown in Fig. 4.

IV. ANALYSIS OF DATA

A. Shift in T_C

The T_C of nanowires shows a clear decrease compared to the bulk and there is a well defined dependence of the T_C on the diameter d as can be seen from Fig. 4. One of the ways in which the dependence of T_C on d can be described is by the finite size scaling laws.[14] The finite size effect can be observed as a change in T_C when the correlation length $\xi(T)$ is comparable to or larger than diameter d. The asymptotic behavior of the correlation length $\xi(T)$ of a magnetic system close to the bulk transition temperature is described by[14]

$$\xi(T) = \xi_0|t|^{-\nu}, \tag{1}$$

where ξ_0 is the extrapolated value of $\xi(T)$ at $T=0$ K and $t = \frac{T-T_c}{T_c}$ is the reduced temperature. The critical temperature T_C for a wire of diameter d scales with the diameter of the nanowires as

$$\frac{T_C(\infty) - T_C}{T_C(\infty)} = \left(\frac{\xi_0}{d}\right)^{\lambda} \tag{2}$$

where, $T_C(\infty)$ is the T_C of the bulk. The finite size scaling exponent can be related to the correlation function exponent ν as $\lambda = 1/\nu$. The exponent can also be determined by the order parameter exponent as we discuss later on. The fit to the equation is shown in Fig. 4. We obtain $\lambda = 0.98$. The value obtained from the results of resistivity anomaly agrees very well with those obtained from magnetization measurements ($\lambda = 0.94$) for nanowires.[7] However it is lower than the values predicted by three-dimensional (3D) Heisenberg model ($\lambda = 1.4$) and 3D Ising model ($\lambda = 1.58$).[5,18] The value of $\xi_0 (= 3.35$ nm), obtained from the fit, is larger than but compares reasonably well with that derived from the magnetization measurements[7] (which is 2.2 nm). The departure of the observed λ from the theoretical predictions is discussed later on. Though we do not commit at this stage that the shift in T_C due to size reduction is only due to the finite size scaling, however, such an explanation has a physical basis in the size range of the nanowires. We explore this again in the discussion section.

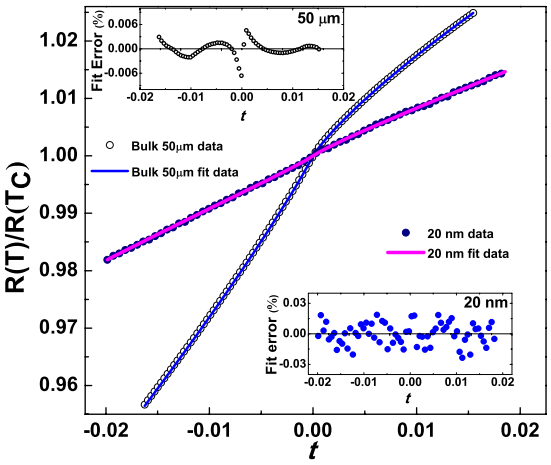

FIG. 5. (Color online) $\frac{R(T)}{R(T_C)}$ vs t (along with the fits) for the 20 nm and bulk wire about T_C (t=0). The insets show the percentage error for bulk and 20 nm diameter nanowire data fits.

B. Analysis of the resistance anomaly near T_C

We now investigate the issue of whether the resistance anomaly near T_C can indeed be analyzed using the framework of critical phenomena, at least operationally. We do not put forward any theoretical arguments whether such analysis is justifiable but instead investigate empirically whether such an approach can be used. In nanowires such issues like strain as well as other effects can lead to a rounding-off of the transition and we would have to address this issue while analyzing the data in the critical region. The resistivity data near T_C in bulk Ni wires have been adequately analyzed by precision experiments in two earlier reports and they are well accepted values for the critical exponents.[11,12] To standardize our analysis methodology, we use the data of the 50 μm thick bulk Ni wire and analyze it using the protocol as described earlier,[11,12] in the region around T_C for $|t| \leq 10^{-2}$. We use the equation,

$$R(t) = R_0 + R't + \begin{cases} A_-|t|^{(1-\alpha_r)}(1 + D_-|t|^z) & (t < 0), \\ A_+t^{(1-\alpha_r)}(1 + D_+t^z) & (t \geq 0). \end{cases} \quad (3)$$

The terms R_0 and $R't$ mainly consist of the noncritical part of the resistance of the sample. The third term is the critical part of the resistance responsible for the power law behavior. This is the part that gives rise to the resistance anomaly. α_r is the critical exponent with A_- and A_+ being the critical amplitudes of the leading term. We note that in the framework of the Fisher-Langer theory,[10] α_r is the same as the specific heat exponent α. This has been validated in experiments with bulk materials. However, this need not be the case in nanowires. Since we do not know whether this identity is valid in such systems of reduced dimension, we use the exponent α_r instead. Z is the exponent and D_- and D_+ are the amplitudes of the second order correction to scaling or the confluent singularity. Z=0.55 as predicted by the renormalization group theory.[19] Though Eq. (3) represents the behavior of resistance near T_C for a homogeneous material with no spread in T_C, one can correct for the inhomogeneities by using a convolution of the form[11,12]

$$R^*(T,T_C,\sigma) = \int R(T,T_C - x)g_\sigma(x)dx, \quad (4)$$

where $g_\sigma(x)$ is a Gaussian in x of width σ and x is the temperature variance from an average T_C. In the region very close to T_C there is a deviation due to rounding-off which is discussed later on. The integration was numerically solved using a 32-point Gauss-Hermite quadrature and a least-square fitting was done with parameters R_0, R', α, A_-, A_+, D_-, D_+, T_c, and σ with a maximum fit error of 0.04%. A typical fit for the bulk wire is shown in Fig. 5 with the fitting error shown in the top inset. The values of the fit exponents obtained by us for the 50 μm thick bulk Ni wire data agree very well with previous high precision data on Ni near the critical point.[11,12] We analyzed the data near T_C for wires of different diameters. We note that even for the 20 nm diameter nanowire, the data can be fitted to Eq. (4) with accuracy which is comparable to that obtained for the bulk data (as shown in Fig. 5). For the other nanowires also the fits are similar and are not shown to avoid duplications. The extracted parameters for all the wires are tabulated in Table II along with the exponents obtained from the previous work on Ni bulk samples.

In Fig. 6, we show a plot of the derivative of resistivity $\frac{d\rho(T)}{dT}$ as a function of the reduced temperature t for nanowires of different diameters. The data have been plotted for a region very close to T_C. It can be seen that there is a clear decrease in the maximum value of $\frac{d\rho(T)}{dT}$ as d is decreased but the existence of the critical region even in the 20 nm wire is visible.

TABLE II. The exponents for the bulk and the nanowires obtained by fitting.

Reference/diameter (nm)	T_C (K)	α_r	A_+/A_-	D_+/D_-	σ
Bulk Ref. 11	630.284 ± 0.003	−0.095 ± 0.002	−1.53 ± 0.02	−0.8 ± 0.1	0.13 ± 0.12
Bulk Ref. 12	630.650 ± 0.450	−0.089 ± 0.003	−1.48 ± 0.03	−1.2 ± 0.2	1.28 ± 0.03
50000	630.248 ± 0.001	−0.0996 ± 0.0001	−1.506 ± 0.001	−0.981 ± 0.031	0.141 ± 0.007
200	617.752 ± 0.003	−0.0864 ± 0.0006	−1.423 ± 0.013	−0.845 ± 0.028	0.435 ± 0.025
100	606.903 ± 0.017	−0.081 ± 0.001	−1.382 ± 0.021	−0.737 ± 0.148	0.321 ± 0.001
55	590.004 ± 0.008	−0.0638 ± 0.0005	−1.290 ± 0.012	−0.103 ± 0.022	0.445 ± 0.018
20	520.339 ± 0.011	−0.0309 ± 0.0001	−1.003 ± 0.002	0.466 ± 0.048	0.521 ± 0.016

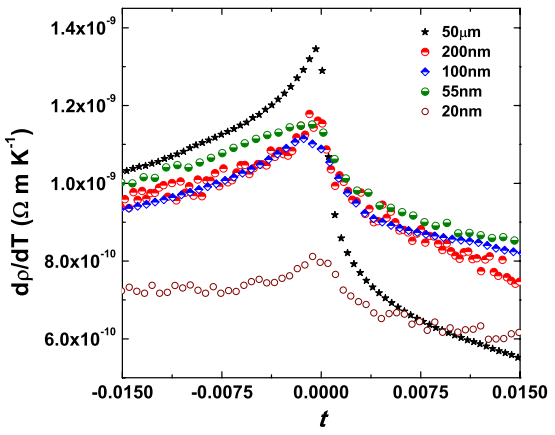

FIG. 6. (Color online) $\frac{d\rho(T)}{dT}$ as a function of t for nanowires of different diameters.

The above analysis establishes that the resistivity anomaly exists in ferromagnetic nanowires (down to 20 nm) at their transition temperature T_C. However, the anomaly and the associated critical behavior is progressively suppressed. The exponents and other parameters obtained form the analysis above, show a very clear trend as the diameter is reduced (see Table II). In Fig. 7 we show a plot of α_r as a function of $1/d$. In case of the nanowires, there is a considerable decrease in the absolute magnitude of α_r showing a slowing down of the growth of the derivative $\frac{d\rho}{dT}$ near the critical point. In addition, changes in the amplitude ratios A_+/A_- and D_+/D_- are also prominent (see Fig. 7).

V. DISCUSSIONS

A. Confinement and strain effects

The critical behavior observed can be affected by the strain and also by strain inhomogeneities. In this section we discuss these issues with quantitative estimates as they can affect our experiments. While uniform strain can produce a

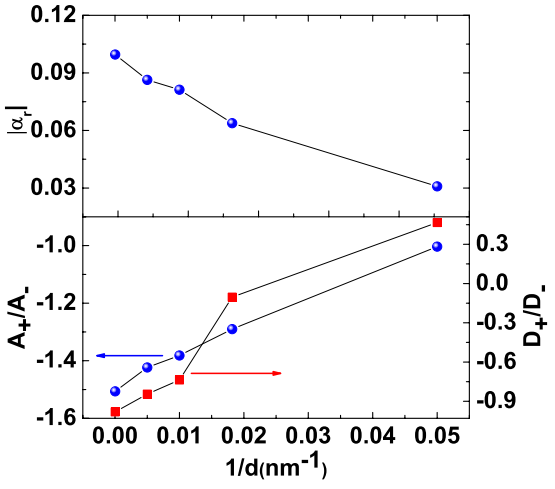

FIG. 7. (Color online) Variation in $|\alpha_r|$ and amplitude ratios A_+/A_- and D_+/D_- for the wires studied as determined from the scaling relation [Eq. (4)].

shift in T_C, the anisotropic strain may affect the resistance anomaly because the fluctuations that make the resistance anomaly near T_C can get affected if the strain is more along one direction. The inhomogeneous strain will lead to strain broadening of the transition, which can also come from the distribution of sizes of the nanowires due to pore size distribution of the template in which they were grown. While analyzing the data near the critical point the rounding-off becomes an important issue. This is present even in bulk systems such as Ni and in nanowires, in particular, when we do the measurements in an array of nanowires, these can be substantial. Thus we would like to estimate the region around T_C that will get affected by the rounding-off and would like to leave out this region from the evaluation of exponents.

Equation (4), which has been used to fit the data, also gives us the width σ of the temperature distribution T_C that can lead to rounding-off of the transition. The values of σ are given in Table II. The bulk samples and the 50 μm thick bulk wire have low but finite σ (<0.15 K). This increases for nanowires and for the thinnest wires it is ≤ 0.5 K. Thus, a region of $T_C \pm 1$ K will be affected by rounding-off. We see below that estimates based on different methods give us similar numbers.

The strain due to confinement can lead to two effects: (a) it can modify the critical region because of magnetoelastic effects and (b) it can change the transition temperature T_C through strain dependence of T_C which can be anisotropic as well as inhomogeneous. The inhomogeneous strain will lead to rounding-off of the transition region. Below we analyze them with quantitative estimate.

The strain through magnetoelastic effect can produce an effective anisotropy energy that can compete with shape anisotropy energy which is the dominant anisotropy energy in these materials. The magnetostriction constant $\lambda_{striction}$ for polycrystalline Ni is large near room temperature ($\approx -35 \times 10^{-6}$), this however, $\rightarrow 0$ as $T \rightarrow T_C$. In the temperature range where the resistance anomaly has been studied, $|\lambda_{striction}| < 3 \times 10^{-6}$. We estimate below that confinement can produce a stress that is < 1 GPa. For a stress of 1 GPa, the maximum magnetoelastic energy density $\approx 0.3 \times 10^4$ J m^{-3}. This is much smaller compared to the shape anisotropy energy[8] $\approx 9.5 \times 10^5$ J m^{-3}. Thus, near the transition, the strain effects through the magnetoelastic coupling cannot produce any appreciable effect that can affect the critical region because $\lambda_{striction} \rightarrow 0$ as $T \rightarrow T_C$. This effect thus can be neglected.

It can be seen from Table I that the strain inhomogeneity in the wires so grown are $\approx 4 \times 10^{-3}$ for wires with diameter ≥ 100 nm and $\approx 7 \times 10^{-3}$ for smaller wires. Using these values of microstrain, we can estimate the expected maximum spread in δT_C of the transition temperature due to strain inhomogeneity using the bulk modulus of Ni (180 GPa) and the dependence of T_C on pressure ($\frac{dT_C}{dP} \approx 1.9$ K/GPa).[12] We get $\delta T_C \approx \pm 0.75$ K for the wires with diameter ≥ 100 nm and $\approx \pm 1$ K for the wires with smaller diameters. The above analysis provides us with an estimate of maximum spread that one would expect for the T_C from strain inhomogeneity. It can be seen that this matches very well with σ obtained from the fit to the data. From the above analysis it can be seen that the critical behavior near T_C will be

rounded-off in an approximate range of ± 1 K around T_C. Thus to avoid the effect of rounding-off, we have left out the data in the region $|t| < 2 \times 10^{-3}$ in the estimation of the exponents.

Confining the wire within the template can cause strain that may be anisotropic due to differential thermal expansion between the alumina template (thermal expansion coefficient $\alpha_{th} = 6 \times 10^{-6}$ K^{-1}) and the Ni nanowires ($\alpha_{th} \approx 13 \times 10^{-6}$ K^{-1}). In addition, the ends are on Ag epoxy that has $\alpha_{th} = 18 \times 10^{-6}$ K^{-1}. The nanowires have lengths of ≈ 50 μm which is the thickness of the membranes. The Ni wires, if they do not adhere to the walls of the templates will have a tensile lateral strain, due to the expansion coefficient mismatch with the Ag end connections and Ni. The magnitude of the strain will be $\approx 1.75 \times 10^{-3}$ for temperatures close to T_C. There will be an associated compressive axial strain $\approx 0.53 \times 10^{-3}$ (using Poisson's ratio of Ni ≈ 0.3). If the nanowires adhere to the walls of alumina, they will have a tensile lateral strain of $\approx 4.2 \times 10^{-3}$ and using Poisson's ratio of alumina ≈ 0.23, we get an axial compressive strain $\approx 0.97 \times 10^{-3}$. One would thus expect a tensile lateral strain lying in the range $\approx (0.5-4) \times 10^{-3}$ and a compressive strain in the range $\approx (0.5-1) \times 10^{-3}$. These strains will lead to stresses $\approx 0.1-0.8$ GPa for the tensile stress and $\approx 0.1-0.2$ GPa for the compressive stress (using Young modulus of Ni = 200 GPa). In any case the strain due to thermal expansion mismatch will be well within 1 GPa. Using $\frac{dT_C}{dP} \approx 1.9$ K/GPa, we find that the shift in T_C that can arise from the tensile strain/compressive strain is < 2 K. Thus confinement effects cannot produce the large shift in T_C that we observe on size reduction.

B. Suppression of T_C on size reduction

The suppression of T_C on size reduction can be due to finite size effect. Other sources that can produce reduction are impurities that expand the lattice, thus reducing the effective interaction strength, or negative pressure/tensile strain, which can also reduce T_C. The nanowires used in this experiment are of very high purity. Thus impurity is not expected to play a role. The estimation of strains in Sec. V A has shown that strain cannot have such a substantial effect that it can shift the T_C by more than 100 K. In view of this, we can consider finite size effect as the predominant agent for the reduction in T_C. The effect of finite size can be appreciable in the temperature and size regime we are working in. As the transition temperature is approached, the correlation length gets constrained by the wire diameter. The correlation length $\xi(t)$ diverges near the transition temperature following Eq. (1).

In Fig. 8, we show the estimated correlation length $\xi(t)$ as obtained from Eq. (1) for nanowires using exponent λ and ξ_0 obtained from the shift in T_C data from the resistance and magnetization measurements on nanowires. In the same graph we show the corresponding data obtained on polycrystalline thin films. In the graph we mark the diameters of the wires used by us. It thus appears that for wires below 200 nm, in the temperature range we have analyzed the data for critical behavior ($|t| \leq 0.02$), the correlation length is larger than or comparable to the wire diameter. Thus one may expect the finite size effect to set in.

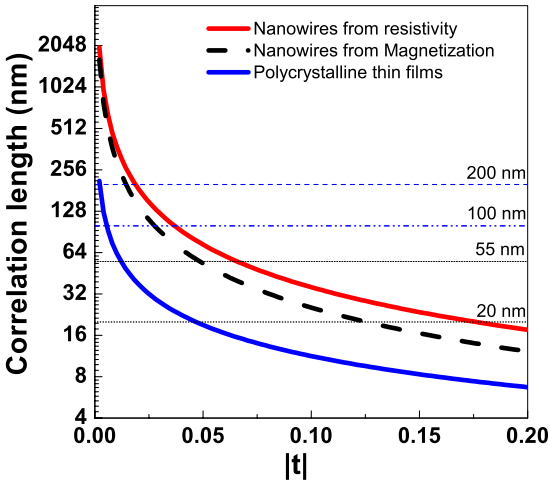

FIG. 8. (Color online) Truncation of correlation length by the wire diameters; resistance anomaly (this work); magnetization (Ref. 7); and polycrystalline thin films (Ref. 6).

The value of λ as obtained from the finite size shift of T_C [Eq. (2)], is close to 1. This is smaller than what one would expect from the relation $\lambda = 1/\nu \approx 1.4-1.5$.[14] However, it has been argued,[20] that in addition to the fact that λ determined by the correlation length exponent ν, there are additional contributions in finite size scaling, which make in d dimension $\lambda = (d-2) + \eta$, where η is the order parameter correlation function exponent, which for a Heisenberg model is ~ 0.04. This depends on the geometry of the system. In Table III, we list the values of λ from experiments done on films using determination of T_C from resistivity methods and also on Ni nanowires where T_C was determined from the magnetization data. λ obtained from high purity Ni film is $= 1.01 \pm 0.11$,[6] which is close to what we have also obtained experimentally. This is also close to $\lambda = 0.94$ obtained on Ni nanowires from magnetization measurements. From Table III, it is observed that in both Ni films and nanowires $\lambda \approx 1$ is common. From the available data it thus seems that the exponent of T_C shift follows the relation $\lambda = (d-2) + \eta$ with $\eta = 0.04$, as stated earlier.

C. Suppression of amplitude of the critical scattering

One of the principal observations of this investigation is the change in the critical scattering that gives rise to the

TABLE III. Value of λ obtained by different findings.

Reference	Technique used	λ
21	Theory for thin films	1
22	Spin polarization measurements on ultrathin films	1.03
7	Magnetization in nanowires	0.94
6	Resistance anomaly in thin films	1.01
This work	Resistance anomaly in nanowires	0.98

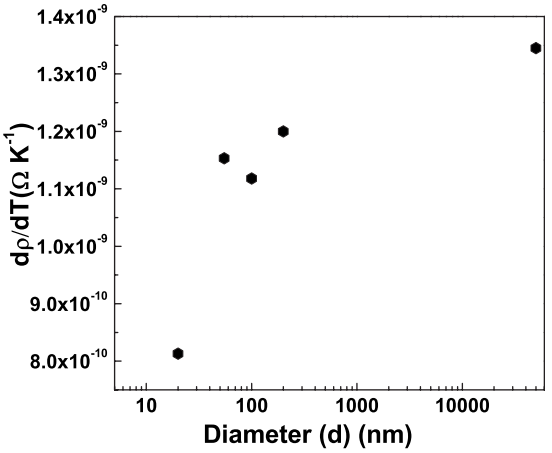

FIG. 9. Variation in $[\frac{d\rho(T)}{dT}]_{\max}$ with wire diameter as determined from resistive anomaly.

resistivity anomaly in Ni nanowires near T_C. The above analyses have clearly shown that the function as given in the Eq. (3) at least can describe the electrical resistivity close to T_C. There is a gradual change from the bulk values as the size is reduced. A very important prediction of the scaling theory of finite size effect relates to the size dependence of the amplitude of the physical quantity that becomes critical at T_C.[14] This important prediction of finite size scaling regarding the amplitude $\frac{d\rho(T)}{dT}$ at $t=0$ (which we will denote as $[\frac{d\rho(T)}{dT}]_{\max}$) has been investigated in Ni films and a logarithmic dependence on thickness has been found.[6] For the derivative like $\frac{d\rho(T)}{dT}$ one would expect from the finite size scaling that the size dependence of $[\frac{d\rho(T)}{dT}]_{\max}$ will follow a size dependence of the type $\sim L^{\alpha/\nu}$, where L is the measure of the size. Since α is small, this dependence is experimentally indistinguishable from the logarithmic dependence as has been seen in precision experiments on Ni films.[6] It is noted that although there are investigations of finite size effects in ferromagnetic nanowires through shift of T_C, there are no reported data on size dependence of $[\frac{d\rho(T)}{dT}]_{\max}$. In Fig. 9, we show the variation in the amplitude of $[\frac{d\rho(T)}{dT}]_{\max}$ with the diameter d. There appears to be an approximate logarithmic dependence as one would expect from the finite size scaling theory. However, the dependence is not perfect. There can be reasons for this departure. The value of $[\frac{d\rho(T)}{dT}]_{\max}$ contains a small contribution from the $\frac{d\rho(T)}{dT}$ from the noncritical part. This varies as d is changed. Thus there is a small but finite component in $[\frac{d\rho(T)}{dT}]_{\max}$ that will not follow scaling law and it is different for wires of different diameters. The amplitude will also be modified partly by the strain inhomogeneity which is not the same for all the samples. Keeping in mind this limitation, the variation in $[\frac{d\rho(T)}{dT}]_{\max}$ with diameter d of the nanowire appears to be a manifestation of finite size effect.

VI. SUMMARY

In summary, using precision measurements of electrical resistance of nickel nanowires of various diameters (down to 20 nm), we have explored the resistance anomaly at the critical point as the size is reduced to an extent that correlation length is truncated by the finite wire diameter. The data analysis establishes that the observed resistance anomaly shows critical behavior down to the lowest diameter wire of 20 nm although with suppressed amplitude. The anomaly close to T_C can be treated in the existing framework of resistance behavior near a critical region although the exponents and amplitudes change as d is reduced. We find that the magnitude of the exponent α_r decreases continuously from the bulk value as d is reduced. This shows that the critical behavior is suppressed upon size reduction. With the decrease in diameter, we observed a decrease in the transition temperature T_C, as observed in magnetic measurements. There is also a suppression of the derivative $[\frac{d\rho(T)}{dT}]_{\max}$ as d is reduced. Both these phenomena are analyzed in the framework of finite size effects at the critical region.

ACKNOWLEDGMENTS

The authors thank the Department of Science and Technology, Govt. of India and CSIR, Govt. of India for financial support in the form of a Unit and sponsored scheme. M.V.K. acknowledges CSIR, Govt. of India. DST Unit for nanoscience and technology, IACS, Kolkata, India is acknowledged for providing TEM support.

*Present address: IPCMS, Department of Magnetic Objects on the Nanoscale, 23 rue du Loess BP 43, F-67034, Strasbourg Cedex 2, France; venkata@ipcms.u-strasbg.fr

†arup@bose.res.in

[1] A. Bid, A. Bora, and A. K. Raychaudhuri, Phys. Rev. B **74**, 035426 (2006).

[2] M. V. Kamalakar and A. K. Raychaudhuri, Phys. Rev. B **79**, 205417 (2009).

[3] A. Bid, A. Bora, and A. K. Raychaudhuri, Phys. Rev. B **72**, 113415 (2005).

[4] M. Venkata Kamalakar, A. K. Raychaudhuri, X. Wei, J. Teng, and P. D. Prewett, Appl. Phys. Lett. **95**, 013112 (2009).

[5] H. E. Stanley, *Introduction to Phase Transition and Critical Phenomena* (Oxford University Press, New York, 1971).

[6] H. Lutz, P. Scoboria, J. E. Crow, and T. Mihalisin, Phys. Rev. B **18**, 3600 (1978).

[7] L. Sun, P. C. Searson, and C. L. Chien, Phys. Rev. B **61**, R6463 (2000).

[8] P. M. Paulus, F. Luis, M. Kröll, G. Schmid, and L. J. de Jongh, J. Magn. Magn. Mater. **224**, 180 (2001).

[9] S. Samanta, M. Venkata Kamalakar, and A. K. Raychaudhuri, J. Nanosci. Nanotechnol. **9**, 5243 (2009).

[10] M. E. Fisher and J. S. Langer, Phys. Rev. Lett. **20**, 665 (1968).

[11] O. Källbäck, S. G. Humble, and G. Malmström, Phys. Rev. B

24, 5214 (1981).
[12] D. L. Decker and W. Chen, Phys. Rev. B **46**, 8237 (1992).
[13] D. S. Simons and M. B. Salamon, Phys. Rev. B **10**, 4680 (1974).
[14] M. E. Fisher and M. N. Barber, Phys. Rev. Lett. **28**, 1516 (1972).
[15] M. Venkata Kamalakar and A. K. Raychaudhuri, Adv. Mater. **20**, 149 (2008).
[16] M. Venkata Kamalakar, Ph.D. thesis, Jadavpur University, Kolkata, India, June, 2009.
[17] G. K. Williamson and W. H. Hall, Acta Metall. **1**, 22 (1953).
[18] C. M. Schneider, P. Bressler, P. Schuster, J. Kirschner, J. J. de Miguel, and R. Miranda, Phys. Rev. Lett. **64**, 1059 (1990).
[19] J. C. Le Guillou and J. Zinn-Justin, Phys. Rev. B **21**, 3976 (1980); Phys. Rev. Lett. **39**, 95 (1977).
[20] C. Domb, J. Phys. A **6**, 1296 (1973).
[21] R. Zhang and R. F. Willis, Phys. Rev. Lett. **86**, 2665 (2001).
[22] H. J. Elmers, J. Hauschild, H. Höche, U. Gradmann, H. Bethge, D. Heuer, and U. Köhler, Phys. Rev. Lett. **73**, 898 (1994).